

RESEARCH ARTICLE | SEPTEMBER 27 2023

# Impact of the oxidation temperature on the density of single-photon sources formed at SiO<sub>2</sub>/SiC interface

Mitsuaki Kaneko ; Hideaki Takashima ; Konosuke Shimazaki ; Shigeki Takeuchi ; Tsunenobu Kimoto 



*APL Mater.* 11, 091121 (2023)  
<https://doi.org/10.1063/5.0162610>

 CHORUS



CrossMark



**APL Machine Learning**  
**Latest Articles Online!**  
**Read Now**



# Impact of the oxidation temperature on the density of single-photon sources formed at SiO<sub>2</sub>/SiC interface

Cite as: APL Mater. 11, 091121 (2023); doi: 10.1063/5.0162610

Submitted: 15 June 2023 • Accepted: 7 September 2023 •

Published Online: 27 September 2023



View Online



Export Citation



CrossMark

Mitsuaki Kaneko,<sup>1,a)</sup> Hideaki Takashima,<sup>1,2</sup> Konosuke Shimazaki,<sup>1</sup> Shigeki Takeuchi,<sup>1</sup> and Tsunenobu Kimoto<sup>1</sup>

## AFFILIATIONS

<sup>1</sup>Department of Electronic Science and Engineering, Kyoto University, Kyoto 615-8510, Japan

<sup>2</sup>Chitose Institute of Science and Technology, 758-65 Bibi, Chitose 066-8655, Japan

<sup>a)</sup>Author to whom correspondence should be addressed: [kaneko@semicon.kuee.kyoto-u.ac.jp](mailto:kaneko@semicon.kuee.kyoto-u.ac.jp)

## ABSTRACT

The impact of oxidation temperature on the formation of single photon-emitting defects located at the silicon dioxide (SiO<sub>2</sub>)/silicon carbide (SiC) interface was investigated. Thermal oxidation was performed in the temperature range between 900 and 1300 °C. After oxidation, two different cooling processes—cooling down in N<sub>2</sub> or O<sub>2</sub> ambient—were adopted. Single photon emission was confirmed with second-order correlation function measurements. For the samples cooled in an N<sub>2</sub> ambient, the density of interface single photon sources (SPSs) increased with decreasing oxidation temperature with a density that could be controlled over the 10<sup>5</sup> to 10<sup>8</sup> cm<sup>-2</sup> range. For the O<sub>2</sub> cooled samples, on the other hand, many interface SPSs were formed irrespective of the oxidation temperature. This is attributed to the low-temperature oxidation during the cooling process after oxidation.

© 2023 Author(s). All article content, except where otherwise noted, is licensed under a Creative Commons Attribution (CC BY) license (<http://creativecommons.org/licenses/by/4.0/>). <https://doi.org/10.1063/5.0162610>

## I. INTRODUCTION

A single photon source (SPS) is recognized as one of the most promising key components to realize quantum sensing and quantum cryptography. Some point defects in wide bandgap semiconductors are known to exhibit single photon emission and are known as “color centers.” They have several advantages compared to fluorescence of a wide range of quantum systems (e.g., trapped ions, single molecules, and carbon nanotubes), such as room temperature operation and integration with semiconductor devices. The negatively charged nitrogen-vacancy in diamonds emits single photons at room temperature and is widely acknowledged as the most investigated and advanced color center.<sup>1–3</sup> Silicon carbide (SiC) also harbors color centers, and the negatively charged silicon vacancy (V<sub>Si</sub><sup>-</sup>) receives much attention.<sup>4–8</sup> Controlling the spin of a single V<sub>Si</sub><sup>-</sup> has been reported.<sup>9</sup> Although such color centers are promising, one of the disadvantages is their relatively low brightness and low spin contrast. SPSs also exist at the interface of silicon dioxide (SiO<sub>2</sub>) and

SiC, and they exhibit photons at least an order of magnitude brighter than the other color centers in SiC.<sup>10–14</sup> However, the defect structure of the interface SPS has not been clarified and its density is not well controlled. Since the interface SPSs can be easily formed by thermal oxidation, the formation process of thermal oxides differs from one laboratory to another, leading to a poor understanding of the interface SPSs.

In this study, the impact of oxidation temperature on the density of the interface SPS was investigated. The density of the interface SPSs can be controlled over a broad range from 10<sup>5</sup> to 10<sup>8</sup> cm<sup>-2</sup> by simply changing the oxidation temperature. The samples oxidized at low temperatures include high densities of the interface SPS. The similarity in the oxidation temperature dependence of the interface SPS to that of the interface states near the conduction band edge indicates that the origin of the interface SPSs is likely a carbon-related defect. In addition to that, defects at the SiO<sub>2</sub>/SiC interface play an important role as not only SPSs for quantum technology but scattering centers in a metal–oxide–semiconductor field-effect tran-

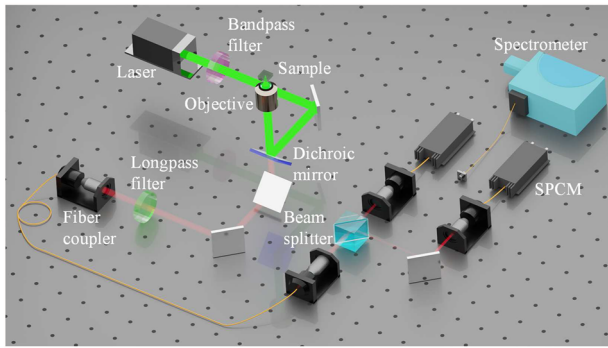


**FIG. 1.** Experimental setup. Laser light is focused using an objective lens. The fluorescence collected with the objective lens is analyzed using the single-photon counting modules or the spectrometer.

sistor for power electronics. Since the interface SPSs originate from some kinds of  $\text{SiO}_2/\text{SiC}$  interface defects, several research groups have recently proposed that the photoluminescence (PL) mapping for the interface SPSs can be an alternative method to characterize the interface quality.<sup>13,15,16</sup> From this point of view, the relationship between the SPS density and interface state density ( $D_{it}$ ) obtained in this study is also briefly discussed.

## II. EXPERIMENTS

High-purity semi-insulating 4H-SiC(0001) substrates grown by high-temperature chemical vapor deposition were used in this study. The substrates were dipped in  $\text{H}_2\text{SO}_4 + \text{H}_2\text{O}_2$ ,  $\text{HCl}$ ,  $\text{HCl} + \text{HNO}_3$ , and  $\text{HF}$  solutions. Then, the substrates were rinsed in de-ionized water and loaded into an oxidation furnace. The furnace temperature was raised to the oxidation temperature at a ramping rate of  $20^\circ\text{C}/\text{min}$  with an  $\text{O}_2$  gas flow. The oxidation temperature was changed from  $900$  to  $1300^\circ\text{C}$ . The oxidation time varied in the range of  $5$  min to  $20$  h. After the thermal oxidation, we adopted two different cooling processes: (i) cooling down in  $\text{O}_2$  ambient ( $\text{O}_2$  cooling) and (ii) changing the gas flow from  $\text{O}_2$  to  $\text{N}_2$  before cooling ( $\text{N}_2$  cooling). The cooling rate was  $5^\circ\text{C}/\text{min}$  for both cooling processes. The  $\text{SiO}_2$  thickness was in the range of  $2$  to  $35$  nm, which was measured by spectroscopic ellipsometry.

The optical experimental setup consisted of a stage scanning confocal microscope, as shown in Fig. 1.<sup>17,18</sup> The excitation laser was a continuous-wave laser ( $\lambda = 532$  nm), and the laser power was  $6$ – $9$  mW before an objective lens. Note that the defects characterized and analyzed in this study are limited to those accessible by the  $532$ -nm laser. When a laser with another wavelength is used, different defects can be measured.<sup>10</sup> The samples were mounted on a three-axis piezo actuator and scanned at a step size of  $200$  nm with an objective lens with a numerical aperture of  $0.9$ . The luminescence from the samples was collected with the same objective lens and measured by a

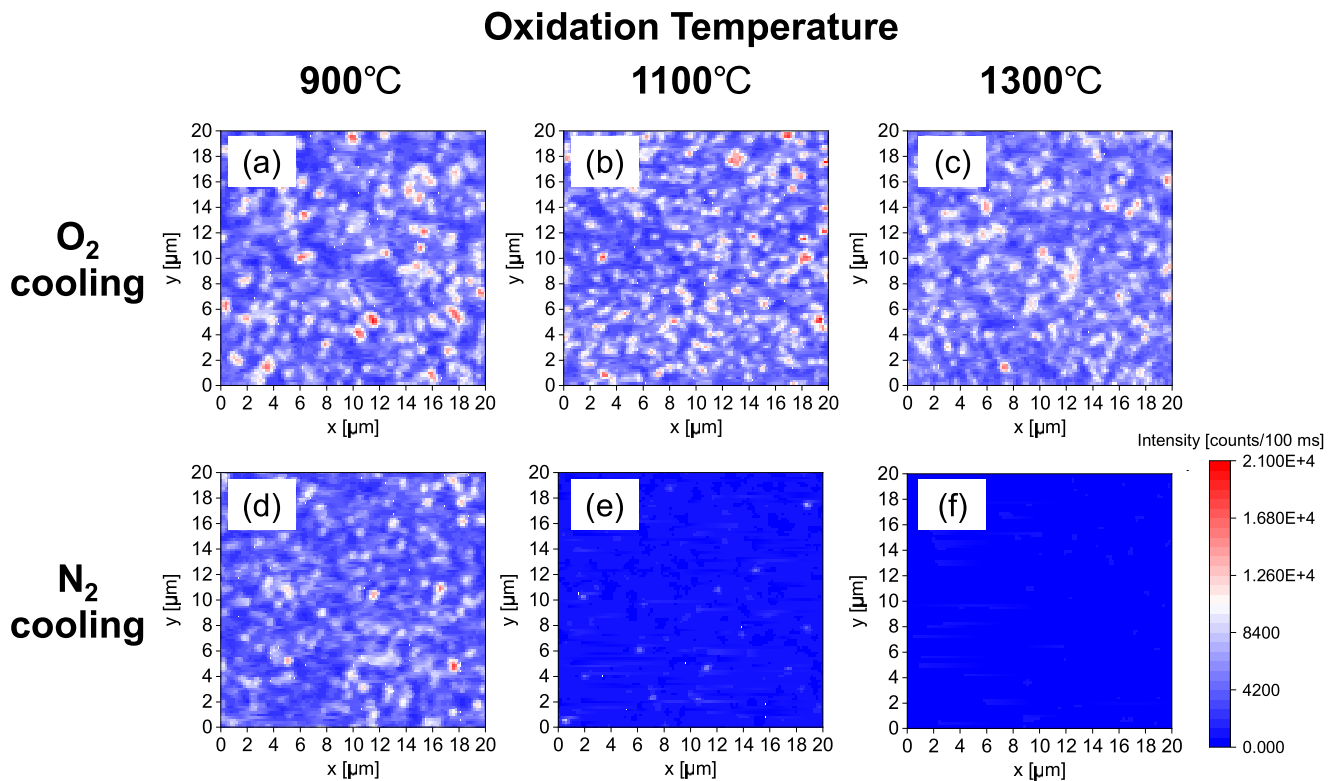


**FIG. 2.** Confocal scanning images ( $20 \times 20 \mu\text{m}^2$ ) of the SiC samples oxidized at the temperatures of  $900$ ,  $1100$ , and  $1300^\circ\text{C}$  with (a)–(c)  $\text{O}_2$  cooling and (d)–(f)  $\text{N}_2$  cooling.

single-photon counting module (SPCM) or a spectrometer equipped with a charge coupled device camera. The second-order correlation function  $g^2(\tau)$  was also measured using two SPCMs. In order to cut the excitation light, a 575 or 600-nm long-pass filter was placed in front of the multi-mode fiber with a core diameter of about 10  $\mu\text{m}$  (SMF-28) to propagate the photons to the SPCMs or the spectrometer, respectively. We manually counted the number of bright spots in the PL mapping image. Note that a bright spot may include more than one SPS when SPSs are located within the diffraction-limited volume. All measurements were performed at room temperature.

We also prepared n-type 4H-SiC (0001) epilayers with a donor density of  $1 \times 10^{17} \text{ cm}^{-3}$  on n-type substrates to form metal-oxide-semiconductor capacitors. The n-type epilayers were chemically cleaned and oxidized at 1300 °C at the same time as the semi-insulating substrates were oxidized. After the oxidation, circular Al electrodes were deposited (diameter: 300–500  $\mu\text{m}$ ). The quasi-static and 1 MHz capacitance-voltage measurements were performed to extract the  $D_{it}$ .

### III. RESULTS

Figure 2 shows confocal scanning images of the samples oxidized at temperatures of 900, 1100, and 1300 °C. Figures 2(a)–2(c) and 2(d)–2(f) are acquired from the samples with O<sub>2</sub> cooling and N<sub>2</sub> cooling, respectively. In the case of O<sub>2</sub> cooling, lots of bright spots

are confirmed and no significant difference can be seen among the samples oxidized at the different oxidation temperatures. On the other hand, bright spots remarkably decreased with elevating the oxidation temperature for the N<sub>2</sub> cooled samples [Figs. 2(d)–2(f)]. We did not observe any single bright spots from the sample oxidized at 1300 °C with N<sub>2</sub> cooling even when the scanning area was expanded to 50  $\times$  50  $\mu\text{m}^2$ .

The second-order correlation function  $g^2(\tau)$  of bright spots in the samples oxidized at 1100 °C with O<sub>2</sub> cooling and N<sub>2</sub> cooling is depicted in Figs. 3(a) and 3(b), respectively. Note that the experimental data were normalized and corrected in the way described in Ref. 19. A dip at around zero delay is not clearly obtained from the sample with O<sub>2</sub> cooling. The bright spot of the sample with O<sub>2</sub> cooling may consist of a few SPSs owing to its high density [Fig. 2(b)]. On the other hand, from the sample with N<sub>2</sub> cooling, a sharp dip is observed, meaning that well isolated SPSs were formed. The red curve shown in Fig. 3(b) shows the fitting result using a three-level model.<sup>20</sup> The  $g^2(0)$  is estimated to be 0.2, which is less than 0.5. Then, bright spots observed in the scanning images are regarded as interface SPSs. Note that one main reason why  $g^2(0)$  is not zero even for the fitting result is due to the timing jitter of the photon detectors.<sup>21</sup> The photoluminescence (PL) spectra from bright spots in the samples oxidized at 1100 °C with O<sub>2</sub> cooling and N<sub>2</sub> cooling are shown in Figs. 3(c) and 3(d), respectively. The spectra exhibit wide variability in the emission peaks. Note that the peaks include zero-phonon lines and phonon sidebands. The peak wavelength is in the range

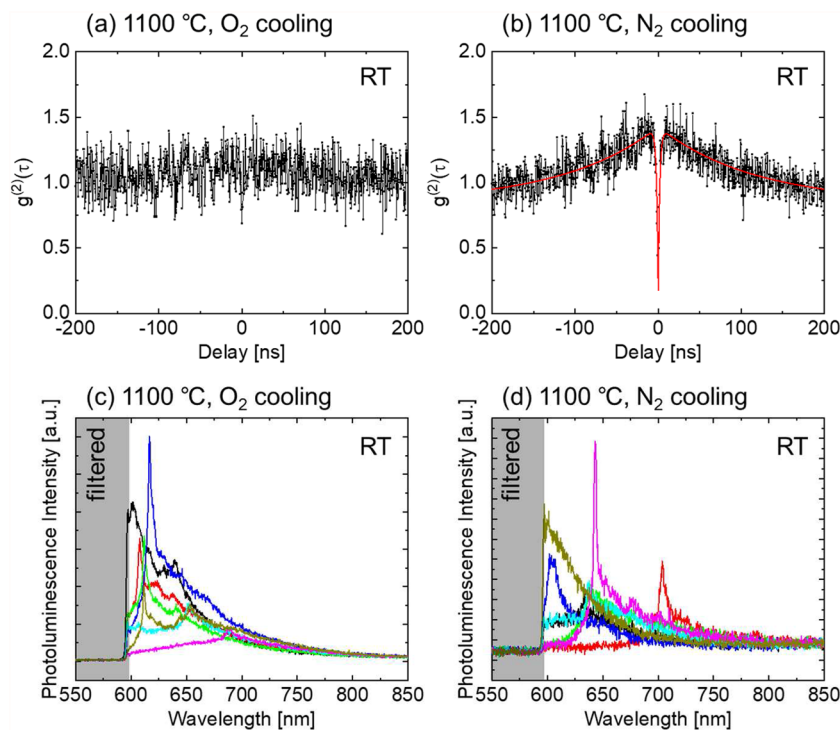


**FIG. 3.** A second-order correlation function  $g^2(\tau)$  of bright spots in the samples oxidized at 1100 °C with (a) O<sub>2</sub> cooling and (b) N<sub>2</sub> cooling. The red curve shown in (b) represents the fitting result using a three-level model. Examples of photoluminescence spectra from bright spots in the sample oxidized with (c) O<sub>2</sub> cooling and (d) N<sub>2</sub> cooling.

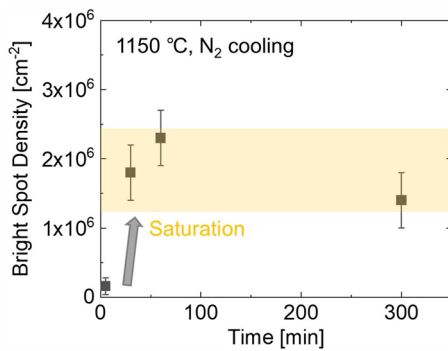


FIG. 4. Dependence of bright spot density on oxidation time at the oxidation temperature of 1150 °C.

between 600 and 750 nm, which is consistent with previous studies using an excitation laser with a wavelength of 532 nm.<sup>12,13</sup> Many peaks in the PL spectra from the O<sub>2</sub> cooling sample are detected, whose number is larger than that from the N<sub>2</sub> cooling sample, supporting that  $g^2(0)$  becomes unity in the O<sub>2</sub> cooling sample [Fig. 3(a)] due to several SPSs located at bright spots within the excitation volume of the laser.

Figure 4 depicts the oxidation time dependence of the bright spot density. The oxidation was performed at a temperature of

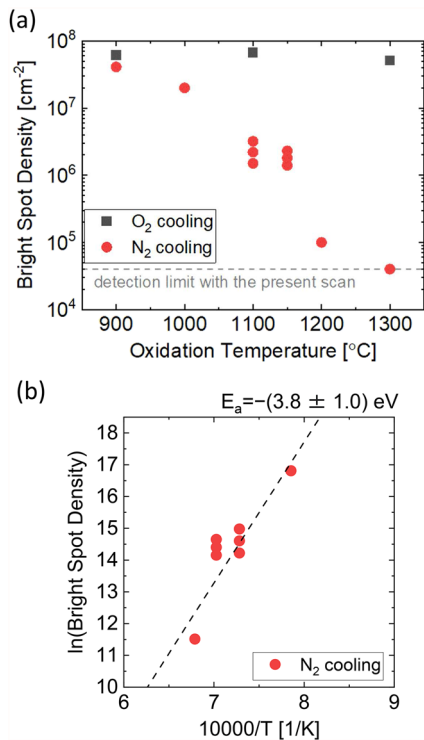


FIG. 5. (a) Bright spot density vs oxidation temperature in the SiO<sub>2</sub>/SiC structure. Black squares and red circles represent the samples with O<sub>2</sub> cooling and N<sub>2</sub> cooling, respectively. (b) Arrhenius plot of the bright spot density (N<sub>2</sub> cooling).

1150 °C with N<sub>2</sub> cooling, and the oxidation time varied from 5 to 300 min. The bright spot density does not strongly depend on the oxidation time and reaches around  $2 \times 10^6 \text{ cm}^{-2}$  except for the sample that was oxidized for 5 min. The relatively low density of the 5-min oxidation sample is attributed to the very short oxidation time (SiO<sub>2</sub> thickness: 3 nm). Bright spot density saturates at a certain value soon after oxidation proceeds.

The oxidation temperature dependence of the bright spot density is shown in Fig. 5(a). As shown in Figs. 2(a)–2(c), the bright spot density of the samples with O<sub>2</sub> cooling is high and does not depend on the oxidation temperature. On the other hand, the bright spot density of the samples with N<sub>2</sub> cooling dramatically decreases with elevating the temperature and control of the bright spot (interface SPS) density in the range from  $10^5$  to  $10^8 \text{ cm}^{-2}$  is achieved by changing the oxidation temperature.

#### IV. DISCUSSION

First, we discuss why the bright spot (interface SPS) density does not vary depending on the oxidation temperature for the samples with O<sub>2</sub> cooling. During the cooling period after the oxidation with an O<sub>2</sub> gas flow, oxidation at the SiO<sub>2</sub>/SiC interface slightly proceeds. The bright spot density in the samples with O<sub>2</sub> cooling was close to that in the sample oxidized at the lowest temperature (900 °C) with N<sub>2</sub> cooling. According to previous studies, the SiC(0001) surface is known to be oxidized at 900 °C, whereas oxidation hardly proceeds at 800 °C.<sup>22</sup> Considering that all the samples with O<sub>2</sub> cooling were slightly oxidized at 900 °C or lower during the cooling process, the present result suggests that the bright spot density is determined by the temperature at which the oxidation takes place at last, regardless of what temperature the sample was previously oxidized at. To examine this hypothesis, we prepared a SiC sample oxidized at a low temperature (900 °C) with O<sub>2</sub> cooling and subsequently oxidized the SiC at a high temperature (1300 °C) with N<sub>2</sub> cooling. Confocal scanning images of this sample (not shown) revealed that bright spots, whose density was consistent with the density extracted from Fig. 2(a) (900 °C, O<sub>2</sub> cooling), were formed at the first oxidation step, and they were removed by the next high-temperature oxidation, which clearly indicates that the bright spot density is determined by the oxidation condition performed at last.

The defect structure of SPSs at a SiO<sub>2</sub>/SiC interface has not been identified yet, and we briefly discuss the origin of the SPSs. A SiO<sub>2</sub>/SiC interface works as a channel of a SiC metal–oxide–semiconductor field-effect transistor, which is of importance as a next generation power device to reduce energy loss, and intensive research has been done to investigate defects at the SiO<sub>2</sub>/SiC interface.<sup>23</sup> It has been reported that unintentional oxidation during cooling down after oxidation introduces interface states whose density is higher than that in the sample without oxidation during the cooling process.<sup>24</sup> Reference 24 reported that the  $D_{it}$  (and flat band shift) does not depend on the oxidation temperature for the samples oxidized with O<sub>2</sub> cooling. The reason for a lower density of interface states in the sample oxidized without unintentional oxidation during cooling down was explained by favorable out-diffusion of CO<sub>x</sub>, whereas excess carbon atoms remained at the SiO<sub>2</sub>/SiC interface when low-temperature oxidation occurred.

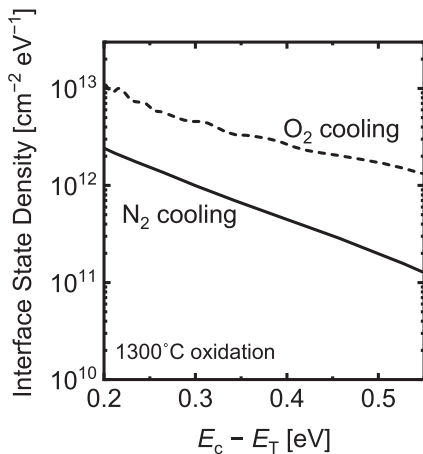


**FIG. 6.** Energy distribution of the interface state density of the sample oxidized at 1300 °C with O<sub>2</sub> and N<sub>2</sub> cooling extracted by the high (1 MHz)-low method.

High-temperature oxidation effectively reduces such excess carbon-related defects (interface states).<sup>25</sup> The energy distributions of the  $D_{it}$  estimated by a high (1 MHz)-low method are given in Fig. 6. The lower  $D_{it}$  was obtained from the sample oxidized with N<sub>2</sub> cooling, which is the same trend given in the literature.<sup>24</sup> Taking account of the similarity between the temperature dependence of the  $D_{it}$  and the bright spot density, the SPSs observed in this study may originate from carbon-related defects. Figure 7 illustrates excitation and emission polarization measurements of bright spots observed at the SiO<sub>2</sub>/SiC interface. As previously reported,<sup>11,26</sup> we also confirmed that the interface SPSs measured in this study hold emission and absorption dipoles that are aligned with the SiC lattice, indicating that the defects are located on the SiC side (not in the oxide layer). First-principles calculations predict that dicarbon antisites (defects), which are located on the SiC side, are easily introduced by low-temperature oxidation and form multiple energy levels inside the energy bandgap of SiC.<sup>27,28</sup> Such a carbon-related defect is a possible origin of the interface SPSs. Note that the Arrhenius plot of the bright spot density [Fig. 5(b)] yields the activation energy of  $-(3.8 \pm 1.0)$  eV, which is close to the absolute value of the activation energy of the SiO<sub>2</sub> growth rate (2.9 eV).<sup>24</sup> The removal rate of the SPSs, or the reduction rate of the excess carbon-related defects, may be determined by the oxidation rate.

The origin of the SPS interface is a controversial issue. Hijikata *et al.* proposed that oxygen-vacancy defects are the possible origin of the interface SPSs by comparing their experimental results with the *ab initio* study.<sup>14</sup> Although we believe that the results obtained in this study can be explained by considering the origin of the interface SPSs as carbon-related defects, our study does not exclude oxygen-vacancy defects as a candidate for the origin of the interface SPSs. Further studies are required to clarify the specific defect structure of the interface SPS.

As briefly discussed in the Introduction, PL mapping receives attention as a technique to characterize the SiO<sub>2</sub>/SiC interface quality. Woerle *et al.* reported that the interface SPS density depends on the  $D_{it}$ , which was electrically measured.<sup>15</sup> In this study, the higher  $D_{it}$  was obtained from the sample with the highest SPS density

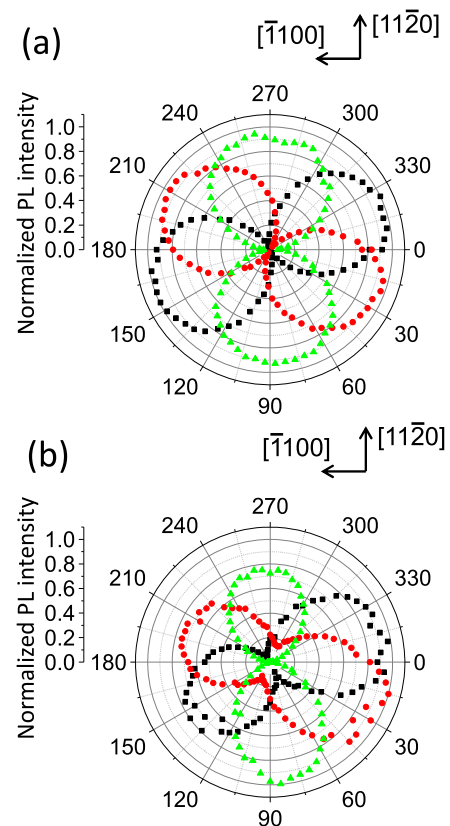


**FIG. 7.** (a) Excitation and (b) emission polarization measurements of three bright spots observed at the SiO<sub>2</sub>/SiC interface. The red, blue, and yellow dots show the measurement results for different bright spots.

(1300 °C with O<sub>2</sub> cooling) compared with the sample with almost no SPSs (1300 °C with N<sub>2</sub> cooling), which partly agrees with the results given in the literature.<sup>13,15</sup> It is well known that the as-oxidized SiO<sub>2</sub>/SiC interface includes high  $D_{it}$  and post-oxidation annealing in nitric-oxide (NO) effectively reduces  $D_{it}$ . Even for the sample with low SPS density (1300 °C with N<sub>2</sub> cooling) obtained in this study, the  $D_{it}$  is still high compared to that of the NO-annealed SiO<sub>2</sub>/SiC interface.<sup>29</sup> Then, we conclude that a low SPS density indicates that the SiC was oxidized at a high temperature but does not ensure that the  $D_{it}$  is as low as that with NO annealing. Although PL mapping using a confocal microscope could be a noncontact, non-destructive, spatially resolved technique to assess the quality of the SiO<sub>2</sub>/SiC interface, interface states consist of many types of defects and further studies are required to clarify which type of defects can be characterized by the PL mapping method.

## V. CONCLUSION

In this study, the oxidation temperature of SiC was systematically varied and its impact on the density of photon-emitting defects was investigated. For the samples cooled in an N<sub>2</sub> ambient, the bright spot density monotonically decreased with increasing the oxidation temperature and was controlled in the wide range from 10<sup>5</sup> to 10<sup>8</sup>

cm<sup>-2</sup>. The SPSs tended to be formed by oxidation at low temperatures. The similarity between the temperature dependence of the SPS density and that of the SiO<sub>2</sub>/SiC interface state density indicates that the origin of SPSs is likely a carbon-related defect. Identification of the atomistic structure of the defect is required for understanding and controlling the physical properties of the defect.

## ACKNOWLEDGMENTS

We gratefully acknowledge the financial support in the form of Kakenhi Grants-in-Aid (Grant Nos. 21H04444 and 22H01155) from the Japan Society for the Promotion of Science (JSPS) and the MEXT Quantum Leap Flagship Program (MEXT Q-LEAP) (Grant No. JPMXS0118067634). H.T. acknowledges JST, PRESTO Grant No. JPMJPR2257, Japan.

## AUTHOR DECLARATIONS

### Conflict of Interest

The authors have no conflicts to disclose.

### Author Contributions

**Mitsuaki Kaneko:** Conceptualization (lead); Data curation (lead); Formal analysis (lead); Investigation (lead); Project administration (lead); Validation (lead); Visualization (lead); Writing – original draft (lead). **Hideaki Takashima:** Data curation (supporting); Formal analysis (supporting); Investigation (supporting); Methodology (lead); Software (lead); Writing – review & editing (supporting). **Konosuke Shimazaki:** Data curation (supporting); Investigation (supporting); Methodology (supporting); Visualization (lead); Writing – review & editing (supporting). **Shigeki Takeuchi:** Funding acquisition (lead); Resources (lead); Supervision (lead); Writing – review & editing (lead). **Tsunenobu Kimoto:** Funding acquisition (lead); Resources (lead); Supervision (lead); Writing – review & editing (lead).

## DATA AVAILABILITY

The data that support the findings of this study are available from the corresponding author upon reasonable request.

## REFERENCES

- <sup>1</sup>A. Gruber, A. Dräbenstedt, C. Tietz, L. Fleury, J. Wrachtrup, and C. V. Borczyskowski, "Scanning confocal optical microscopy and magnetic resonance on single defect centers," *Science* **276**, 2012–2014 (1997).
- <sup>2</sup>M. Pompili, S. L. N. Hermans, S. Baier, H. K. C. Beukers, P. C. Humphreys, R. N. Schouten, R. F. L. Vermeulen, M. J. Tiggelman, L. dos Santos Martins, B. Dirkse, S. Wehner, and R. Hanson, "Realization of a multinode quantum network of remote solid-state qubits," *Science* **372**, 259–264 (2021).
- <sup>3</sup>R. Schirhagl, K. Chang, M. Lorez, and C. L. Degen, "Nitrogen-vacancy centers in diamond: nanoscale sensors for physics and biology," *Annu. Rev. Phys. Chem.* **65**, 83–105 (2014).
- <sup>4</sup>H. Kraus, D. Simin, C. Kasper, Y. Suda, S. Kawabata, W. Kada, T. Honda, Y. Hijikata, T. Ohshima, V. Dyakonov, and G. V. Astakhov, "Three-dimensional proton beam writing of optically active coherent vacancy spins in silicon carbide," *Nano Lett.* **17**, 2865–2870 (2017).

- <sup>5</sup>M. E. Bathen, A. Galeckas, J. Müting, H. M. Ayedh, U. Grossner, J. Coutinho, Y. K. Frodason, and L. Vines, "Electrical charge state identification and control for the silicon vacancy in 4H-SiC," *Npj Quantum Inf.* **5**, 111 (2019).
- <sup>6</sup>M. Widmann, M. Niethammer, D. Y. Fedyanin, I. A. Khrantsov, T. Rendler, I. D. Booker, J. Ul Hassan, N. Morioka, Y.-C. Chen, I. G. Ivanov, N. T. Son, T. Ohshima, M. Bockstedte, A. Gali, C. Bonato, S.-Y. Lee, and J. Wrachtrup, "Electrical charge state manipulation of single silicon vacancies in a silicon carbide quantum optoelectronic device," *Nano Lett.* **19**, 7173–7180 (2019).
- <sup>7</sup>M. Niethammer, M. Widmann, T. Rendler, N. Morioka, Y.-C. Chen, R. Stöhr, J. U. Hassan, S. Onoda, T. Ohshima, S.-Y. Lee, A. Mukherjee, J. Isoya, N. T. Son, and J. Wrachtrup, "Coherent electrical readout of defect spins in silicon carbide by photo-ionization at ambient conditions," *Nat. Commun.* **10**, 5569 (2019).
- <sup>8</sup>T. Nishikawa, N. Morioka, H. Abe, H. Morishita, T. Ohshima, and N. Mizuochi, "Electrical detection of nuclear spins via silicon vacancies in silicon carbide at room temperature," *Appl. Phys. Lett.* **121**, 184005 (2022).
- <sup>9</sup>M. Widmann, S.-Y. Lee, T. Rendler, N. T. Son, H. Fedder, S. Paik, L.-P. Yang, N. Zhao, S. Yang, I. Booker, A. Denisenko, M. Jamali, S. A. Momenzadeh, I. Gerhardt, T. Ohshima, A. Gali, E. Janzén, and J. Wrachtrup, "Coherent control of single spins in silicon carbide at room temperature," *Nat. Mater.* **14**, 164–168 (2015).
- <sup>10</sup>A. Lohrmann, N. Iwamoto, Z. Bodrog, S. Castelletto, T. Ohshima, T. J. Karle, A. Gali, S. Praver, J. C. McCallum, and B. C. Johnson, "Single-photon emitting diode in silicon carbide," *Nat. Commun.* **6**, 7783 (2015).
- <sup>11</sup>A. Lohrmann, S. Castelletto, J. R. Klein, T. Ohshima, M. Bosi, M. Negri, D. W. M. Lau, B. C. Gibson, S. Praver, J. C. McCallum, and B. C. Johnson, "Activation and control of visible single defects in 4H-, 6H-, and 3C-SiC by oxidation," *Appl. Phys. Lett.* **108**, 021107 (2016).
- <sup>12</sup>Y. Abe, T. Umeda, M. Okamoto, R. Kosugi, S. Harada, M. Haruyama, W. Kada, O. Hanaizumi, S. Onoda, and T. Ohshima, "Single photon sources in 4H-SiC metal-oxide-semiconductor field-effect transistors," *Appl. Phys. Lett.* **112**, 031105 (2018).
- <sup>13</sup>B. C. Johnson, J. Woerle, D. Haasman, C. T.-K. Lew, R. A. Parker, H. Knowles, B. Pingault, M. Atature, A. Gali, S. Dimitrijević, M. Camarda, and J. C. McCallum, "Optically active defects at the SiC/SiO<sub>2</sub> interface," *Phys. Rev. Appl.* **12**, 044024 (2019).
- <sup>14</sup>Y. Hijikata, S. Komori, S. Otojima, Y.-I. Matsushita, and T. Ohshima, "Impact of formation process on the radiation properties of single-photon sources generated on SiC crystal surfaces," *Appl. Phys. Lett.* **118**, 204005 (2021).
- <sup>15</sup>J. Woerle, B. C. Johnson, C. Bongiorno, K. Yamasue, G. Ferro, D. Dutta, T. A. Jung, H. Sigg, Y. Cho, U. Grossner, and M. Camarda, "Two-dimensional defect mapping of the SiO<sub>2</sub>/4H-SiC interface," *Phys. Rev. Mater.* **3**, 084602 (2019).
- <sup>16</sup>J. Woerle, B. C. Johnson, R. Stark, M. Camarda, and U. Grossner, "Fast defect mapping at the SiO<sub>2</sub>/SiC interface using confocal photoluminescence," *Mater. Sci. Forum* **1062**, 389–394 (2022).
- <sup>17</sup>K. Shimazaki, H. Kawaguchi, H. Takashima, T. F. Segawa, F. T.-K. So, D. Terada, S. Onoda, T. Ohshima, M. Shirakawa, and S. Takeuchi, "Fabrication of detonation nanodiamonds containing silicon-vacancy color centers by high temperature annealing," *Phys. Status Solidi A* **218**, 2100144 (2021).
- <sup>18</sup>K. Fukushige, H. Kawaguchi, K. Shimazaki, T. Tashima, H. Takashima, and S. Takeuchi, "Identification of the orientation of a single NV center in a nanodiamond using a three-dimensionally controlled magnetic field," *Appl. Phys. Lett.* **116**, 264002 (2020).
- <sup>19</sup>A. Beveratos, S. Kühn, R. Brouri, T. Gacoin, J.-P. Poizat, and P. Grangier, "Room temperature stable single-photon source," *Eur. Phys. J. D* **18**, 191–196 (2002).
- <sup>20</sup>R. N. Patel, T. Schröder, N. Wan, L. Li, S. L. Mouradian, E. H. Chen, and D. R. Englund, "Efficient photon coupling from a diamond nitrogen vacancy center by integration with silica fiber," *Light: Sci. Appl.* **5**, e16032 (2016).
- <sup>21</sup>H. Takashima, A. Fukuda, K. Shimazaki, Y. Iwabata, H. Kawaguchi, A. W. Schell, T. Tashima, H. Abe, S. Onoda, T. Ohshima, and S. Takeuchi, "Creation of silicon vacancy color centers with a narrow emission line in nanodiamonds by ion implantation," *Opt. Mater. Express* **11**, 1978 (2021).
- <sup>22</sup>T. Kobayashi, T. Okuda, K. Tachiki, K. Ito, Y.-i. Matsushita, and T. Kimoto, "Design and formation of SiC (0001)/SiO<sub>2</sub> interfaces via Si deposition followed by low-temperature oxidation and high-temperature nitridation," *Appl. Phys. Express* **13**, 091003 (2020).

- <sup>23</sup>T. Kimoto and H. Watanabe, “Defect engineering in SiC technology for high-voltage power devices,” *Appl. Phys. Express* **13**, 120101 (2020).
- <sup>24</sup>T. Hosoi, D. Nagai, M. Sometani, Y. Katsu, H. Takeda, T. Shimura, M. Takei, and H. Watanabe, “Ultrahigh-temperature rapid thermal oxidation of 4H-SiC(0001) surfaces and oxidation temperature dependence of SiO<sub>2</sub>/SiC interface properties,” *Appl. Phys. Lett.* **109**, 182114 (2016).
- <sup>25</sup>T. Hosoi, Y. Katsu, K. Moges, D. Nagai, M. Sometani, H. Tsuji, T. Shimura, and H. Watanabe, “Passive–active oxidation boundary for thermal oxidation of 4H-SiC(0001) surface in O<sub>2</sub>/Ar gas mixture and its impact on SiO<sub>2</sub>/SiC interface quality,” *Appl. Phys. Express* **11**, 091301 (2018).
- <sup>26</sup>M. Widmann, M. Niethammer, T. Makino, T. Rendler, S. Lasse, T. Ohshima, J. Ul Hassan, N. Tien Son, S.-Y. Lee, and J. Wrachtrup, “Bright single photon sources in lateral silicon carbide light emitting diodes,” *Appl. Phys. Lett.* **112**, 231103 (2018).
- <sup>27</sup>S. Wang, S. Dhar, S.-r. Wang, A. C. Ahyi, A. Franceschetti, J. R. Williams, L. C. Feldman, and S. T. Pantelides, “Bonding at the SiC–SiO<sub>2</sub> interface and the effects of nitrogen and hydrogen,” *Phys. Rev. Lett.* **98**, 026101 (2007).
- <sup>28</sup>T. Kobayashi and Y.-i. Matsushita, “Structure and energetics of carbon defects in SiC (0001)/SiO<sub>2</sub> systems at realistic temperatures: Defects in SiC, SiO<sub>2</sub>, and at their interface,” *J. Appl. Phys.* **126**, 145302 (2019).
- <sup>29</sup>K. Tachiki, M. Kaneko, and T. Kimoto, “Mobility improvement of 4H-SiC (0001) MOSFETs by a three-step process of H<sub>2</sub> etching, SiO<sub>2</sub> deposition, and interface nitridation,” *Appl. Phys. Express* **14**, 031001 (2021).